

## Waves in Random and Complex Media

ISSN: (Print) (Online) Journal homepage: <https://www.tandfonline.com/loi/twrm20>

# Simulation of blood flow in human arteries as porous media

Mohammed Al-Saad, Sana J. Yassen, Camilo Suarez-Afanador, Ahmed Kadhim AlShara & Ali J. Chamkha

To cite this article: Mohammed Al-Saad, Sana J. Yassen, Camilo Suarez-Afanador, Ahmed Kadhim AlShara & Ali J. Chamkha (2022): Simulation of blood flow in human arteries as porous media, *Waves in Random and Complex Media*, DOI: [10.1080/17455030.2022.2162151](https://doi.org/10.1080/17455030.2022.2162151)

To link to this article: <https://doi.org/10.1080/17455030.2022.2162151>



Published online: 29 Dec 2022.



Submit your article to this journal [↗](#)



Article views: 8



View related articles [↗](#)



View Crossmark data [↗](#)



## Simulation of blood flow in human arteries as porous media

Mohammed Al-Saad<sup>id</sup><sup>a</sup>, Sana J. Yassen<sup>a</sup>, Camilo Suarez-Afanador<sup>b,c</sup>, Ahmed Kadhim AlShara<sup>id</sup><sup>d</sup> and Ali J. Chamkha<sup>e</sup>

<sup>a</sup>Mechanical Department/Engineering College, University of Basrah, Basrah, Iraq; <sup>b</sup>Aix Marseille Université, CNRS, Centrale Marseille, LMA, Marseille, France; <sup>c</sup>Department of Engineering, Institute of Computational Engineering, University of Luxembourg, Luxembourg, Luxembourg; <sup>d</sup>Mechanical Department/Engineering College, University of Misan, Misan, Iraq; <sup>e</sup>Faculty of Engineering, Kuwait College of Science and Technology, Doha, Kuwait

### ABSTRACT

The porous flow model studies the blood flow in a curve shape. This study has addressed simulations of blood flow in a porous media through an elbow artery; two-dimensional (2D), have been investigated. The blood flow is supplied with diameters such as (300 and 500  $\mu\text{m}$ ). The outputs from numerical simulations have presented the details of blood flow patterns and the local distribution of blood flow along the artery. The effects of permeability concerning the variations in the Reynolds number ( $Re = 0.1, 1$  and  $5$ ) and changing porosity levels have been discussed. Different vessel diameters were studied to show the velocity distribution inside the vessel. Results are presented in variations of velocity distributions and local variations of flow rates through the vessel dimensions. Outputs compare with the available data, and a good agreement find. The study potentially evaluates the role of porosity and flow conditions when the body is subject to diseases.

### ARTICLE HISTORY

Received 26 November 2021  
Accepted 19 December 2022

### KEYWORDS

Blood flow; porous media;  
finite volume; CFD;  
Newtonian fluid

## Introduction

Hemodynamics is one of the significant and more extensive systems connecting several structures at different scales in the human body. Studying the circulatory system under normal and pathological conditions is essential for biomechanical engineering. The main objective of biomechanical engineering is to develop high-quality tools enabling a more comprehensive system and its structures. It allows investigation of the complications encountered in cardiovascular diseases, studying alternative surgical procedures, and extrapolating its consequences via simulations. Thanks to the reliability of contemporary computational and physical modeling techniques, computational simulations have become a powerful tool to solve realistic problems in many scientific and engineering fields [1–3], including biomechanical engineering. In particular, computational simulations can replace the experimental tests involving the Earth system and human bodies.

Many researchers are considered blood as a bio-fluid that can behave as Newtonian fluid when it flows through arteries of the human body [4–6]. From state of the art, it is

an appropriate solution to model blood as a Newtonian fluid when it flows in narrow arteries. Some researchers dealt with the flow in narrow arteries as a porous biological flow [7]. Some biological capillaries examined being porous media, which led to building a porous model [8]. The blood flow in the kidneys, lungs, and tiny capillaries is the best example of a porous medium. Further [9], showed that in biological tissues that contain dispersed cells separated by voids, blood perfuses into the tissue cells via blood capillaries, which serve as a porous medium for blood flow.

The mathematical modeling was presented by [10] to treat the blood flow in the narrow arteries as a porous medium. It was shown that the increase in the threshold significantly increases the frictional resistance. Other researchers have considered the porous medium-based energy equations for computing the temperature distribution in the body of tissue phantoms [11]. In general, a porous medium is a material volume that consists of solid material with an interconnected void space that can be simply characterized via the volume fraction of voids immersed in the solid space [9,12,13]. According to mathematical modeling, Darcy law can be defined as a relationship between the velocities of flow to the pressure gradient across the porous medium that most studies have used [14].

In addition, permeability is commonly used as one of the porous medium's parameters, and it represents the measure of the flow conductivity in the porous medium [15]. The tortuosity and curvature of the vessel are essential factors in the interaction between the fluid and the porous medium, causing a hindrance to flow diffusion imposed by local boundaries. Tortuosity is deemed to be essential for medical applications [9]. Although flow concepts in porous media have been extensively used to solve many realistic scientific and engineering problems [16–20], they only found medical applications in recent decades [21,22]. For example, an idealized geometry was used to simulate the blood flow [23,24]. In addition, the aneurysm diverting stent was simulated as a porous medium in the numerical model [25–27]. A numerical analysis was conducted [28] to simulate blood hemodynamics inside the unruptured aneurysm. A coiled aneurysm model represents a porous volume with porosity and permeability corresponding to the size of the coil and compactness value. It is used to study the effect of endovascular embolization. The study results demonstrated that a smaller coil diameter can lead to less flow circulation within the aneurysm. This study uses numerical analysis to get around most of the porous flow's challenges and difficulties. Because prior blood flow studies in porous media had a minimal focus on flow in curves, such as the elbow, this study was conducted to further our understanding of fluid behavior in these kinds of forms that are regarded as porous media.

The objectives of the current study are to simulate blood flow through an elbow artery in a porous medium. This also demonstrates how to flow characteristics will occur inside the vessel's curvature once blood flow has been released. Several parameters to consider include porosity, permeability, blood flow rate within blood vessels, and geometrical diameters. The blood flow model numerical simulations are examined and compared with the experimental results reported in the literature.

## Numerical methodology

Blood flow can be described as a steady-state, unidirectional laminar flow of 2D incompressible viscous fluids. The present simulations have been performed for different sizes of

blood vessel diameters (300-500  $\mu\text{m}$ ). The tube length is assumed to be large enough compared to its diameter. The permeability of porous medium has been considered to vary in function of the distance from the vessel's center in the radial direction. The governing mass equations for solving isothermal fluid flow inside the blood vessels are [29]:

$$\frac{D\rho}{Dt} + \rho \nabla \cdot \mathbf{v} = 0 \quad (1)$$

where  $D, \rho, t, \mathbf{v}$  the fluid parameters are essential derivative, density, time, and velocity vector, respectively.

Meanwhile, the blood inside the porous region has been described using the Darcy–Brinkman equation, as shown by Eq. (2). The terms in Eq. (2) carry the viscous and the form drag interactions between the fluid and the walls.

$$\frac{1}{\varepsilon} \frac{\partial \mathbf{v}}{\partial t} + \frac{1}{\varepsilon^2} \mathbf{v} \cdot (\nabla^2 \mathbf{v}) = \frac{1}{\rho} \nabla P + \frac{\nu}{\varepsilon} \nabla^2 \mathbf{v} + \frac{\mu}{K} \mathbf{v} \quad (2)$$

where  $\mu$  is the dynamic viscosity ( $\text{m}^2\text{s}^{-1}$ ),  $\varepsilon$  is the porosity of the porous medium,  $K(\text{m}^{-2})$  the permeability, and  $P$  pressure of the fluid. The axial velocity gradient is presented along the axis of symmetry. The arterial wall is considered to be fixed.

## Numerical method

The numerical modeling for determining distributions of the hydrodynamics of blood flow inside a vessel as a porous model has been described. This section discusses the numerical modeling aspect according to geometry.

Simulations have been performed using the Finite Volume Method (FVM) software (ANSYS Fluent 15.0). Time step and grid size have been used until convergence is reached. Numerical simulations estimate the impact of the leading parameters such as geometry, permeability, and porosity.

The vessel with a  $90^\circ$  bend was chosen to investigate the effect of vessel geometry on the blood flow. Figure 1 shows the two-dimensional representation of the blood vessel and geometric parameters for the simulations. The boundary conditions and flow parameters were the same as described previously. As illustrated in Figure 2, a coarse mesh was chosen and smoothed until the solution became independent of the number of nodes. As previously mentioned, high accuracy is achieved by selecting a fine mesh discretization while conforming to the convergence requirements, affecting the time needed for each simulation. It was done to ensure that the numerical solution did not depend on the number of grid nodes. The figure illustrates how the center's velocity nearly approximates a constant for a fine mesh. Since it is independent of the number of nodes after 2.1 million nodes, which can be employed in all solutions. For all flow variables, the convergence residuals requirements have been set to  $1 \times 10^{-7}$ .

As presented in the numerical methodology section, some physically reasonable assumptions have been considered through the numerical model. In addition, it was also assumed that the given physical properties remain constant during the process. The simulation parameters are shown in Table 1. It must be noted that the properties of the permeability parameter are used according to the Kozeny equation. (4). The range of

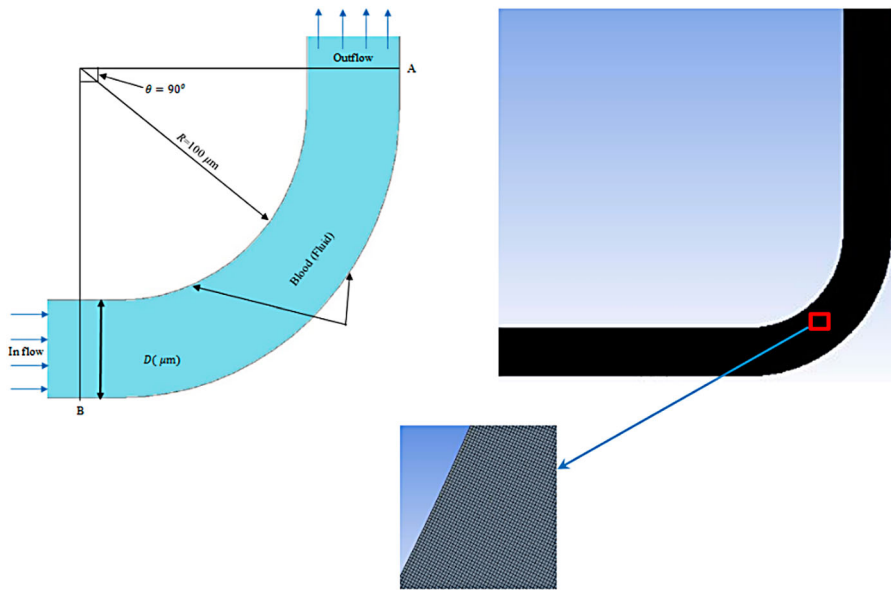


**Figure 1.** The geometry of vessel (90°) with mesh.

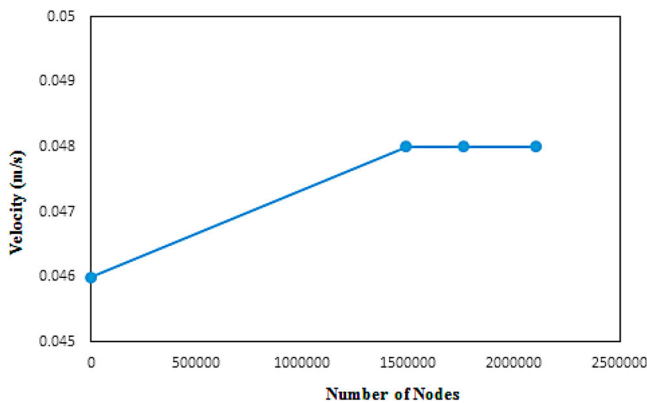


**Figure 2.** Grid independence at different resolutions.

Reynolds numbers is 0.1–5 for blood flow through vessels [30]. Finally, the other numerical values involving parameters are used concerning physiological ranges [31–33]:

$$k = \frac{\phi r^2}{8} \quad (3)$$

The numerical model has been employed to handle the momentum across the porous blood vessel interfaces. A suitable discretization scheme that employs the flow in porous and blood vessel domains has been used.

A good grid arrangement between the grid clustering at the interfaces and the outer walls of the domain has been recommended; meanwhile, physical variables have been

located at the cell center locations of the control volumes. This configuration shows to be suitable for problems involving interfaces between the porous and the fluid flow regions. The model in this work considers a different geometry from which that was reported [34].

**Table 1.** Model parameters and dimensions of vessels.

Porosity	Density (kg/m <sup>3</sup> )	Re	Diameter of the vessel ( $\mu\text{m}$ )	kinematic viscosity (kg/m.s)
0.5–1	1060	0.1–1–5	300–500	0.005

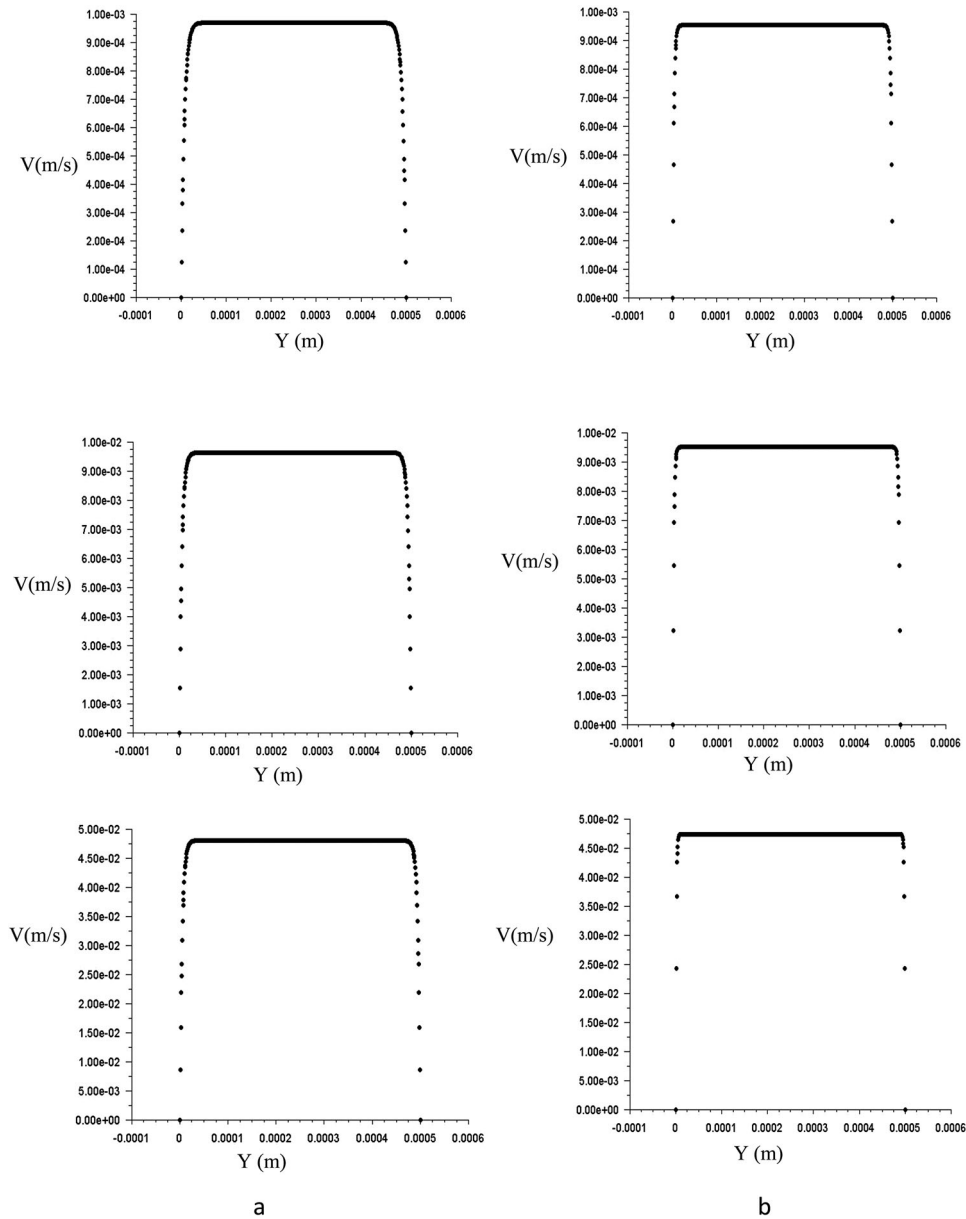


**Figure 3.** Velocity distribution of blood flow for diameter 500  $\mu\text{m}$  and constant permeability. (a) Porosity = 0.5. (b) Porosity = 1. Variable Re (0.1, 1, 5).

The distribution of the velocity profile has been shown for different locations inside the vessel. It shows to be actively dependent on the location applied in the simulation.

For numerical computations, the upstream and downstream vessel length is too long to avoid any distortion at the beginning of the vessel and to keep the fully developed flow [35,36].

## Results and discussion

The numerical solutions are tested under physiological flow conditions. The blood flow simulation results show the effects of parameters such as permeability  $K$ , which depends on eq. (3), Reynolds number, porosity, and bend region were tested to investigate the effect of variable vessel geometry on the fluid flow.

The process of flow can be controlled under some conditions. The steady flow of blood through a porous medium in a vessel, the condition of the wall as a non-slip condition, and considering the blood flow as an incompressible fluid were tested. Also, the artery is represented as a bent tube in 2D.

A detailed geometry diagram showing the length and diameter of the vessel with the fluid region and diameter maintained in every case is pictured in Figure 1. This representation carries the benchmarking for the mass and momentum equations. The blood flow and porous results have been compared with those in the available literature [37]. Uniform flow profiles have been applied at the inlet of the physical domain, and hydrodynamic conditions at the outlet have been assumed.

Flow characteristics when blood flows through vessels in porous medium consideration were studied. The velocity distribution of blood flow using two different values of the porosity factor in the cases of a constant permeability for three different values of Reynolds number is shown in Figure 3(a) and (b), respectively. In the case of constant permeability and the types of porosity, the velocity of blood flow increases as the porosity factor

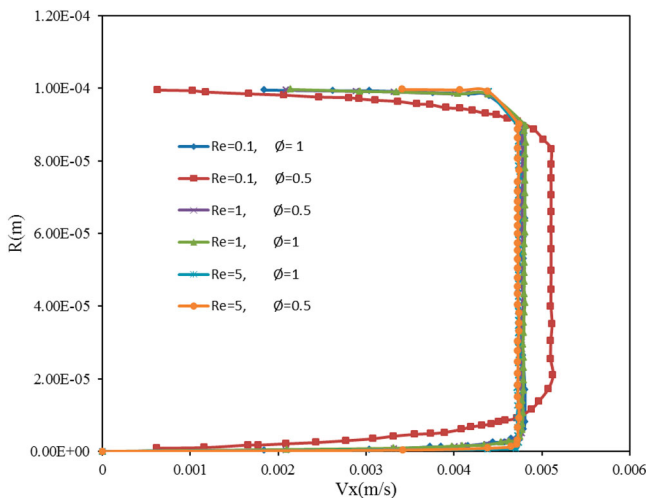


**Figure 4.** Velocity distribution of blood flow for diameter 100  $\mu\text{m}$  different permeability. Variable porosity  $\varepsilon = 0.5, 1$ . Variable Re (0.1, 1, 5).

decreases. Moreover, it is shown from the figures that the magnitude of width of the plug flow region (flatness of the velocity profile) decreases as the porosity factor decreases.

The variation of flow rate for different values of the permeability factor in the cases of constant porosity ( $\varepsilon = 0.5, 1$ ) is shown in Figure 4. In both cases of porosity, the flow rate increases rapidly as the diameter increase from 300 to 500  $\mu\text{m}$ . It is also observed that the variation of pressure gradually increases as the diameter of the vessel increases in the cases of constant porosity ( $\varepsilon = 0.5, 1$ ). In addition, as shown in Figure 5(a,b), the pressure increases as the porosity factor increases.

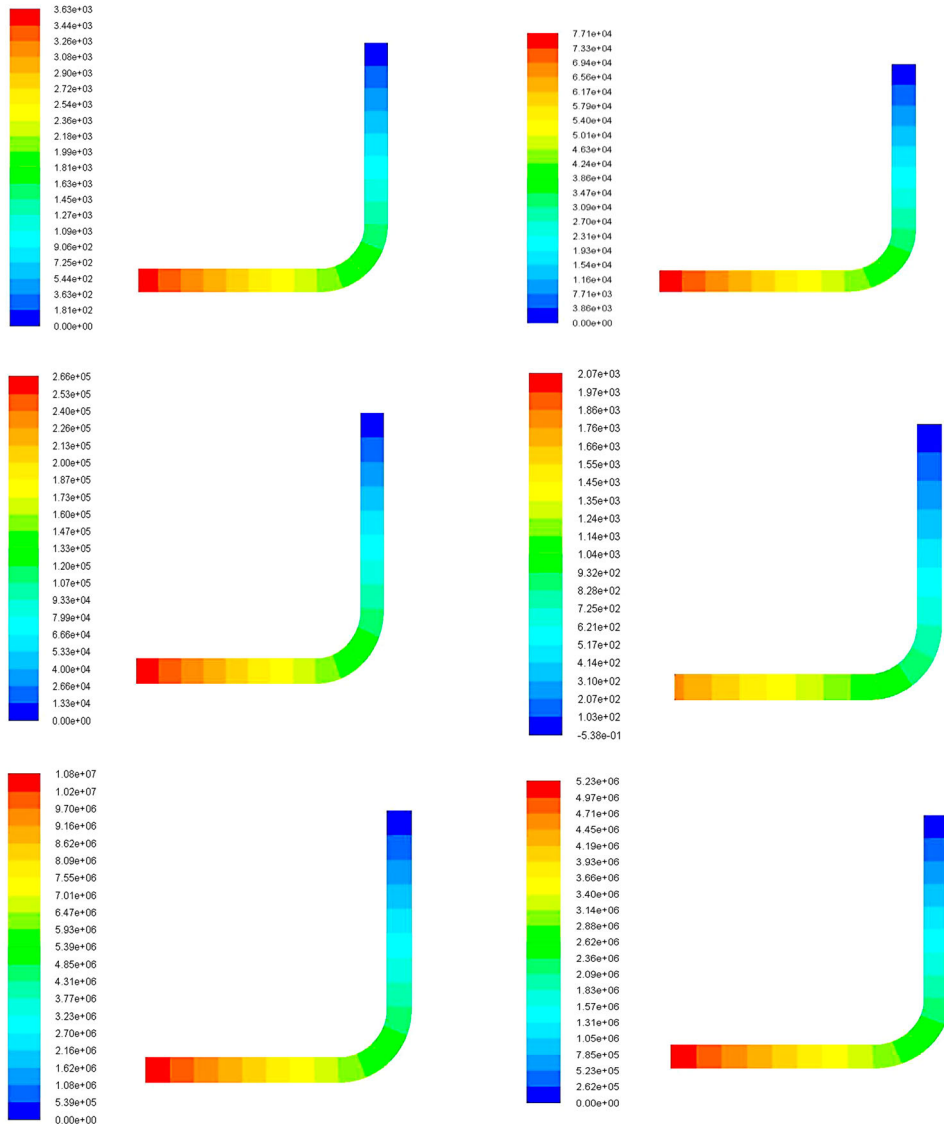


**Figure 5.** Pressure distribution of blood flow for diameter 300  $\mu\text{m}$  constant permeability. (a)  $\varepsilon = 0.5$ . (b)  $\varepsilon = 1$ . Variable Re (0.1, 1, 5).

Figure 6 shows the velocity profiles at two different porosity values. Due to the curvature of the vessel, the velocity cannot be the same as in a straight tube. The maximum velocity will move towards the curvature axis. An increase in porosity will decrease the velocity, and it can move the maximum velocity away from the center [37]. As pointed out [38], the variation of flow velocity increases and accelerates towards the inner diameter of the bent part of the vessel in the cases of constant porosity ( $\varepsilon = 0.5, 1$ ). Furthermore, Figure 5 shows the magnitudes of streamwise velocities to gradually increase with the decrease of Re at the

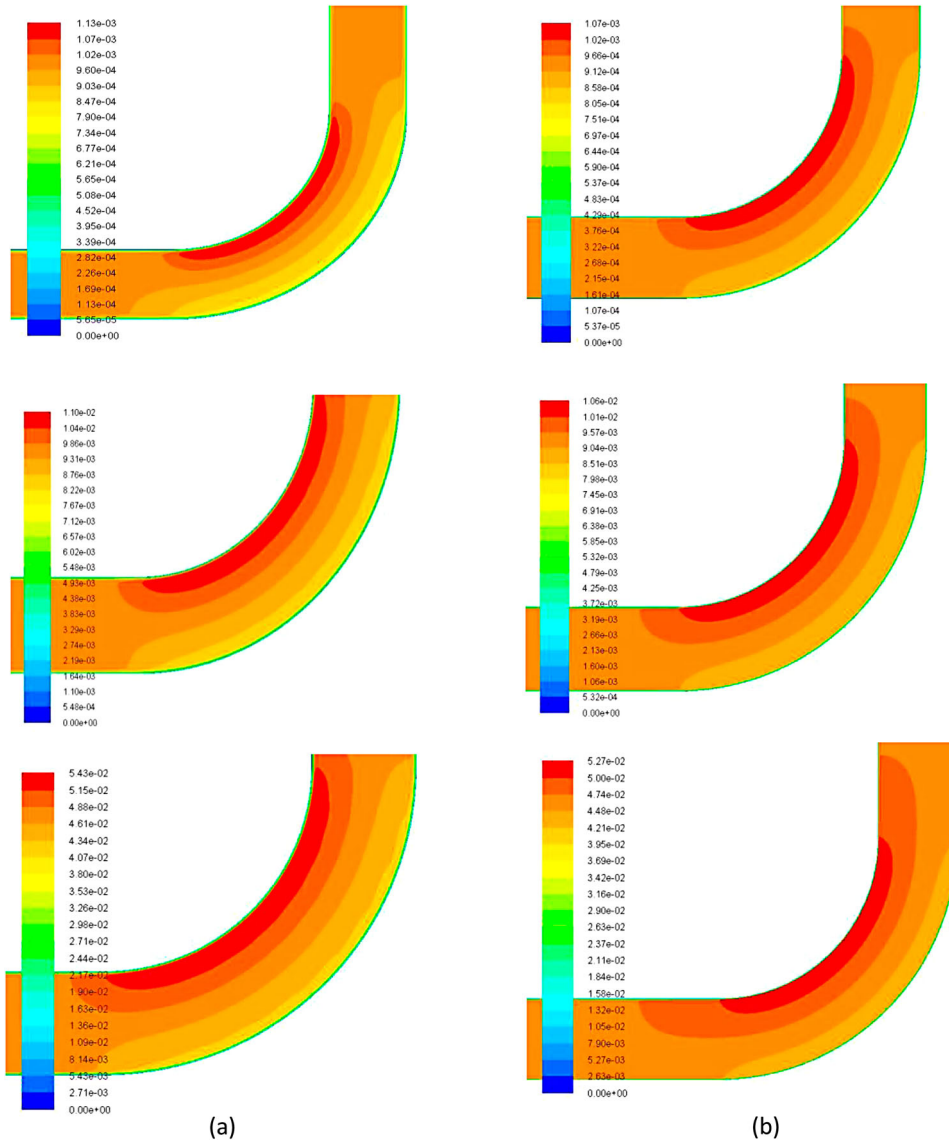


**Figure 6.** Velocity contour in the tube bend at different Re (0.1, 1, 5) for two values of porosity ( $a = 0.5$ ,  $b = 1$ ) at constant diameter = 500  $\mu\text{m}$ .

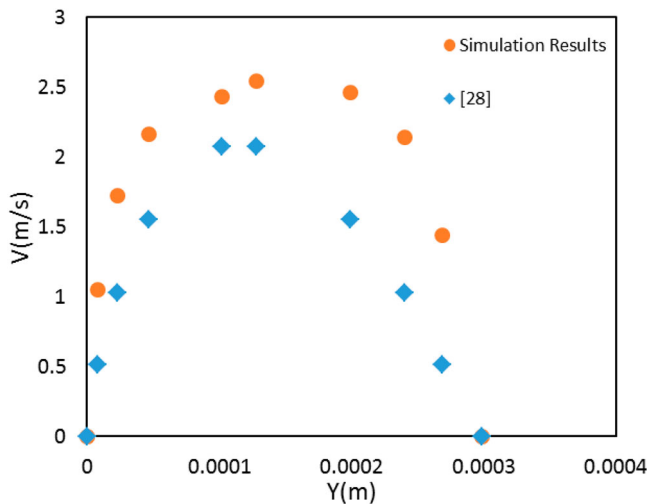


**Figure 7.** Comparison of velocity between simulation results and other researchers for values for  $Re = 1$ , at constant diameter =  $300 \mu\text{m}$ .

bend near the inner diameter. For all  $Re$  cases, the numerical results did not predict a massive increase in the velocity along the bend vessel due to the small values of the Reynolds number (Figure 6).

Figure 7 compares the present numerical simulation results and the literature's most reliable and available results [37]. In the case of  $Re = 1$  and  $D = 300 \mu\text{m}$ , the maximum error is 47% for the peak velocity during the simulation; meanwhile, the error over all domains at steady-state is 18%. Comparing the flow distribution in the vessel does not lead to significant differences, and it gives a good agreement. Despite using a high order of convergence residuals of the numerical scheme and fine grids, numerical errors can affect the results.

## Conclusions

The current study examines blood flow through a porous elbow artery. Other case studies were compared to the findings of the present study. An analysis of blood flow feedback has been conducted by varying Reynolds numbers, porosity, and permeability. Numerical simulations could be used to indicate how the blood flow velocity is influenced in a bend vessel. In addition, assumed penalty values such as different diameters used in the analysis discussed above can be more accurately estimated or calibrated by this study. Finally, the effect of the bend vessel on the blood flow has been examined. It is observed that the magnitude of the velocity profile is changed along with the locations of the vessel. The numerical results also have a good agreement with other reference cases. This study also demonstrates that the hydrodynamics velocity in a bend vessel can also be easily modeled using advanced numerical procedures.

## Disclosure statement

No potential conflict of interest was reported by the author(s).

## ORCID

Mohammed Al-Saad  <http://orcid.org/0000-0002-8061-4998>

Ahmed Kadhim AlShara  <http://orcid.org/0000-0002-8127-3873>

## References

- [1] Zhao C. Dynamic and transient infinite elements: theory and geophysical, geotechnical and geoenvironmental applications. New York: Springer Science & Business Media; 2009.
- [2] Zhao C, Hobbs BE, Ord A. Convective and advective heat transfer in geological systems. New York: Springer Science & Business Media; 2008.
- [3] Zhao C, Hobbs BE, Ord A. Fundamentals of computational geoscience: numerical methods and algorithms. Vol. 122. New York: Springer Science & Business Media; 2009.
- [4] Dash R, Mehta K, Jayaraman G. Effect of yield stress on the flow of a Casson fluid in a homogeneous porous medium bounded by a circular tube. *Appl Sci Res*. 1996;57(2):133–149.
- [5] Sud V, Sekhon G. Arterial flow under periodic body acceleration. *Bull Math Biol*. 1985;47(1):35–52.
- [6] Al-Saad M, Suarez CA, Obeidat A, et al. Application of smooth particle hydrodynamics method for modelling blood flow with thrombus formation. *Comput Model Eng Sci*. 2020;122(3):831–862.
- [7] Guo S, Yu D, Wu W. The physical characteristics of the porous media concerning flow in viscera. *Acta Mech Sin*. 1982;15(1):26–33.
- [8] Mehmood OU, Mustapha N, Shafie S. Unsteady two-dimensional blood flow in porous artery with multi-irregular stenoses. *Transp Porous Media*. 2012;92(2):259–275.
- [9] Khaled A-R, Vafai K. The role of porous media in modeling flow and heat transfer in biological tissues. *Int J Heat Mass Transfer*. 2003;46(26):4989–5003.
- [10] Song F, Xu Y, Li H. Blood flow in capillaries by using porous media model. *J Cent South Univ Technol*. 2007;14(1):46–49.
- [11] Vyas DCM, Kumar S, Srivastava A. Porous media based bio-heat transfer analysis on counter-current artery vein tissue phantoms: applications in photo thermal therapy. *Int J Heat Mass Transfer*. 2016;99:122–140.
- [12] Das B, Batra R. Non-Newtonian flow of blood in an arteriosclerotic blood vessel with rigid permeable walls. *J Theor Biol*. 1995;175(1):1–11.
- [13] Prasad B, Kumar A. Flow of a hydromagnetic fluid through porous media between permeable beds under exponentially decaying pressure gradient. *Comput Methods Sci Technol*. 2011;17(1-2):63–74.
- [14] Eldesoky IM. Slip effects on the unsteady MHD pulsatile blood flow through porous medium in an artery under the effect of body acceleration. *Int J Math Math Sci*. 2012;2012:1–26.
- [15] Misra J, Sinha A, Shit G. Mathematical modeling of blood flow in a porous vessel having double stenoses in the presence of an external magnetic field. *Int J Biomath*. 2011;4(02):207–225.
- [16] Zhao C. Physical and chemical dissolution front instability in porous media. Cham: Springer; 2014.
- [17] Zhao C, Hobbs B, Hornby P, et al. Theoretical and numerical analyses of chemical-dissolution front instability in fluid-saturated porous rocks. *Int J Numer Anal Methods Geomech*. 2008;32(9):1107–1130.
- [18] Zhao C, Hobbs B, Ord A. Theoretical analyses of nonaqueous phase liquid dissolution-induced instability in two-dimensional fluid-saturated porous media. *Int J Numer Anal Methods Geomech*. 2010;34(17):1767–1796.
- [19] Zhao C, Hobbs B, Ord A. Theoretical analyses of acidization dissolution front instability in fluid-saturated carbonate rocks. *Int J Numer Anal Methods Geomech*. 2013;37(13):2084–2105.
- [20] Zhao C, Hobbs B, Ord A. Theoretical analyses of chemical dissolution-front instability in fluid-saturated porous media under non-isothermal conditions. *Int J Numer Anal Methods Geomech*. 2015;39(8):799–820.
- [21] Umeda Y, Ishida F, Tsuji M, et al. Computational fluid dynamics (CFD) using porous media modeling predicts recurrence after coiling of cerebral aneurysms. *PLoS One*. 2017;12(12):e0190222.
- [22] Usmani A, Patel S. Hemodynamics of a cerebral aneurysm under rest and exercise conditions. *Int J Energy Clean Environ*. 2018;19(1-2):119–136.

- [23] Finnigan P, Hathaway A, Lorensen W. Merging CAT and FEM. *Mech Eng.* 1990;112(7):32.
- [24] Taylor CA, Hughes TJ, Zarins CK. Finite element modeling of blood flow in arteries. *Comput Methods Appl Mech Eng.* 1998;158(1-2):155–196.
- [25] Bouillot P, Brina O, Ouared R, et al. Hemodynamic transition driven by stent porosity in sidewall aneurysms. *J Biomech.* 2015;48(7):1300–1309.
- [26] Karmonik C, Anderson J, Beilner J, et al. Relationships and redundancies of selected hemodynamic and structural parameters for characterizing virtual treatment of cerebral aneurysms with flow diverter devices. *J Biomech.* 2016;49(11):2112–2117.
- [27] Li Y, Zhang M, Verrelli DI, et al. Numerical simulation of aneurysmal haemodynamics with calibrated porous-medium models of flow-diverting stents. *J Biomech.* 2018;80:88–94.
- [28] Hamdan MO, Alargha HM, Elnajjar E, et al. Using CFD simulation and porous medium analogy to assess cerebral aneurysm hemodynamics after endovascular embolization. *Proceedings of the 4th World Congress on Momentum, Heat and Mass Transfer (MHMT'19)*, 2019, p. ENFHT 122.
- [29] Fung Y. *Biomechanics: motion, flow, stress, and growth.* Ann Arbor (NY): Edwards Brothers. Inc.; 1990.
- [30] Lyon CK, Scott JB, Anderson DK, et al. Flow-through collapsible tubes at high Reynolds numbers. *Circ Res.* 1981;49(4):988–996.
- [31] Johnson G, Borovetz H, Anderson J. A model of pulsatile flow in a uniform deformable vessel. *J Biomech.* 1992;25(1):91–100.
- [32] Mekheimer KS, El Kot M. Influence of magnetic field and Hall currents on blood flow through a stenotic artery. *Appl Math Mech.* 2008;29(8):1093–1104.
- [33] Taylor D. *Blood flow in arteries.* By DA McDonald. Edward Arnold, London, 1974. *Q J Exp Physiol Cognate Med Sci Transl Integr.* 1975;60(1):65–65.
- [34] Liu Q, Mirc D, Fu BM. Mechanical mechanisms of thrombosis in intact bent microvessels of rat mesentery. *J Biomech.* 2008;41(12):2726–2734.
- [35] Abraham J, Sparrow EM, Tong J. Breakdown of laminar pipe flow into transitional intermittency and subsequent attainment of fully developed intermittent or turbulent flow. *Numer Heat Transfer Part B Fundam.* 2008;54(2):103–115.
- [36] Kays W, Crawford M. *Convective heat and mass transfer.* New York: McGraw-Hill; 1980.
- [37] Wang C. Viscous flow in a curved tube filled with a porous medium. *Meccanica.* 2013;48(1): 247–251.
- [38] Zeng J, Constantinescu G, Blanckaert K, et al. Flow and bathymetry in sharp open-channel bends: experiments and predictions. *Water Resour Res.* 2008;44(9).